Chapter 27
Sedimentation Processes

Ilia Ostrovsky, Yosef Z Yacobi and Nir Koren

Abstract Sedimentation is a major process for removal of particulate material from the water column and an important determinant accounting for the stability of aquatic ecosystems. Gross sedimentation rates (GSRs) in Lake Kinneret (Israel), regularly monitored from 1999 up to date with sedimentation traps, showed salient temporal and spatial variability. In the lake center, the annual mean GSR ranged from 1.9 to 6.0 g m^{-2} day^{-1}. The accumulation rate of sediments at the lake centrum during the study averaged from 2.6 to 4.3 mm $year^{-1}$, in agreement with values obtained by sediment core dating. Organic matter (OM) content comprised 33–42 % of the sinking particulate matter in sediment traps located in the lake center and was 1.5–2 times lesser in peripheral stations. The highest seasonal values of OM content in traps were associated with collapse of algal blooms. Algae and their debris are the main components of OM and their fate in the water column can be well traced by photosynthetic pigments. Chlorophyte signature pigments display much lower degradability in the water column than those of diatoms and dinoflagellates and leave a relatively persistent residue in the buried sediments. Analysis of seasonal changes of algal signature pigments in the upper euphotic zone and those in sedimentation traps allow us to follow the fate of dominant algal phyla in the water column. We argue thatlarge individual algal cells may have better ability to survive in the deep non-stratified water column with limited light, while the ability to retain and recycle in the euphotic epilimnion under conditions of nutrient limitation may well confer an evolutionary advantage to small or buoyant algal populations. Despite large variation in algal community composition, the ratio of OM sedimentation flux to primary production (i.e., the export ratio) alters only slightly throughout the stratified period. Approximately 20 % of the OM supplied to the lake by primary production found its way to the traps. A large decline of water level in recent years affected the processes of particle resuspension and offshore translocation, which caused prominent site-specific impacts on the sedimentation regime. We argue that changes in sedimentation rates observed in the lake are related to fluctuations of loads from the watershed and prominent water-level fluctuations.

I. Ostrovsky (✉) · Y. Z Yacobi · N. Koren
The Yigal Allon Kinneret Limnological Laboratory, Israel Oceanographic
& Limnological Research, P.O. Box 447, 14950 Migdal, Israel
e-mail: ostrovsky@ocean.org.il

Y. Z Yacobi
e-mail: yzy@ocean.org.il

T. Zohary et al. (eds.), *Lake Kinneret, Ecology and Management,* Aquatic Ecology Series 6,
DOI 10.1007/978-94-017-8944-8_27,

Keywords Sedimentation rate · Phytoplankton pigments · Suspended particles · Primary production · Resuspension

Sedimentation is a major process by which particulate material is removed from the water column and an important determinant accounting for the stability of aquatic ecosystems (Håkanson and Jansson 1983; Bloesch 2004). Sedimenting organic particles fuel biogeochemical processes in the hypolimnion and bottom sediments, and determine the burial rate of nutrients and pollutants. Understanding the fate of newly produced particulate organic material (POM) in the water column is one of the fundamental questions in limnology. In the context of organic carbon (OC) cycling, a foremost issue is the proportion of primary production recycled within the upper productive stratum versus the part of this material that is exported to deeper strata, buried in sediments, or removed by other means from the ecosystem (Ostrovsky et al. 1996; Wassmann 2004).

27.1 Gross Sedimentation Rate

Since 1999, gross sedimentation rate (GSR) is regularly monitored in Lake Kinneret with sedimentation traps, moored at stations A, F, and M (for station location see Fig. 32.1 in Chap. 32). GSR has a high spatial and temporal variability (Fig. 27.1).

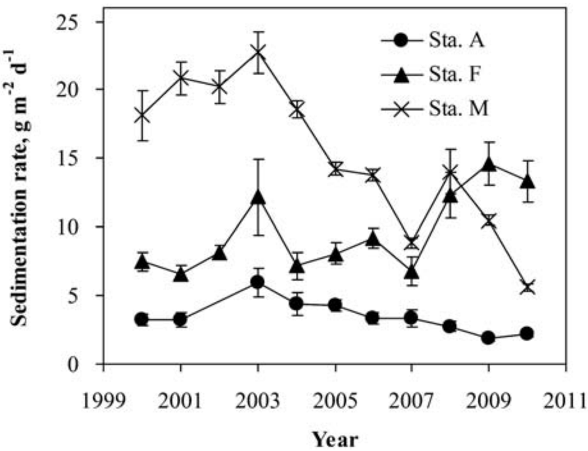

Fig. 27.1 Multiannual variations of the mean (± standard error) gross sedimentation rates in sediment traps positioned ~1.5–2.5 m above the lake bottom ("low traps") at three stations. *Sta. A* is a pelagic station located in the lake center (ca 40-m depth), *Sta. F* is a deep peripheral station (20-m depth), and *Sta. M* is a littoral station (ca 10-m depth). Station locations are indicated in Fig. 32.1, Chap. 32; method details are given in Ostrovsky and Yacobi (2010). In winter 2002–2003 a rapid rise of the water level occurred

Between 2003 and 2010, a 3- to 4-fold decrease in the annual GSR was observed at the lake center (Sta. A, depth 40 m) and at the littoral (Sta. M, 10 m), while an opposite trend was observed at a sublittoral station (Sta. F, 20 m). Since primary production in Lake Kinneret is quite stable (Chap. 24), the decrease in GSR at Sta. A, where resuspension is usually insignificant (Ostrovsky and Yacobi 1999, 2010), suggests notable changes in the rate of POM export from the epilimnion downwards. The observed strong positive correlation between GSR and the maximal annual water level ($r=0.81$, $P<0.01$) or with annual water inflow ($r=0.75$, $P<0.01$) implies that allochthonous particles, imported from the watershed and remaining long term in the water column, affect the sedimentation processes. Another important factor strengthening the correlation between inflows and particle concentration is the external load of nutrients and associated winter–spring dinoflagellate blooms. Over the past two decades, dinoflagellate blooms have been highly correlated with riverine nutrient loads (Zohary and Ostrovsky 2011) and their fluctuations could affect the GSR.

Resuspended materials may contribute up to 80–90 % of the measured GSR at the shallower stations M and F (Ostrovsky and Yacobi 1999, 2010). Therefore, changes in resuspension strongly affect the sedimentation regime at peripheral locations. Since 2001, a conspicuous decrease in GSR has been recorded at the littoral Sta. M ($r=-0.96$, $P<0.001$). This change could be associated with large water-level fluctuations. A progressive decrease in water level exposes large areas of the bottom sediments to energetic surface wave activity, which removes fine particles and redeposits them at deeper locations. As a result, much coarser particles, which are harder to resuspend, become dominant in the littoral. These changes in bottom sediment particle size distribution eventually reduced the contribution of resuspended particles to GSR measured in the shallowest location.

GSR measured at Sta. F was influenced by material transport driven by a combined effect of a fast-deepening thermocline and internal seiching that cause resuspension and redeposition of recently settled fine particles from the shallower area toward the lake center (Ostrovsky and Yacobi 2010). A temporal increase in the annual sedimentation rate at Sta. F ($r=0.73$, $P<0.01$) over the last decade could be associated with processes causing sediment redeposition and focusing in the lake. We suppose that gradual decrease in the mean water level together with enlarged water-level fluctuations were the main driving factors responsible for intensive relocation of finer particles from the littoral and sublittoral areas. One can also speculate that the observed increase in the ratio between lake surface and the epilimnion volume with the decrease in mean water level (Rimmer et al. 2011) leads to more effective transfer of wind energy to the lake boundaries, which should enhance sediment resuspension (Ostrovsky et al. 2006).

Comparison of recent sedimentation trap measurements with previously published data on GSR expressed in units of dry weight (DW) m^{-2} day^{-1} shows conspicuous changes over time (Table 27.1). Most of the data compiled in Table 27.1 are based on measurements made with sedimentation traps placed at Sta. A, 1–2.5 m above the bottom sediments. However, the data for 1990–1996 were collected with traps placed 15.5 and 26 m above the bottom (cf. Nishri and Koren 1993; Koren and Klein 2000). Such positioning is expected to lead to notably lower GSRs than those obtained with near-bottom traps (Ostrovsky and Yacobi 2010). At Sta. A, high

Table 27.1 Mean annual gross sedimentation rate measured with sedimentation traps

Location	Sedimentation rate, g DW m^{-2} day^{-1}	Trap location, m above bottom	Period	Reference
Sta. A	1.8–2.2	1	1972–1973	Serruya et al. (1974); Serruya (1978)
PS	2.5–7.3	1		
Sta. A	3.9–5.6	26	1990–1992	Nishri and Koren (1993)
Sta. A	3.8–5.1	15.5 and 26	1995–1996	Koren and Klein (2000)
PS	4.8–15.2	1.5–2		
Sta. J	22–25	1.5–2		
Sta. A	3.8–6.4	2.5	1999–2000	Eckert et al. (2003)
Sta. A	2.7–6.0	2.5	1999–2008	Present study
Sta. A	1.9–2.2	2.5	2009–2011	Present study
PS	5.2–21.6	1.5	1999–2011	Present study

Sta. A station at the deepest part of the lake (bottom depth of 38–44 m depending on water level), *PS* peripheral stations excluding Sta. J (depth <25 m), *Sta. J* station located south of the Jordan River inlet (depth <10 m)
Station locations are indicated in Fig. 32.1 of Chap. 32

GSRs (4–6 g DW m^{-2} day^{-1}) were observed from the early 1990s to the mid-2000s. The GSRs for 1990–1996, collected for near-bottom locations, could be even larger than numbers presented in Table 27.1. Much lower values of ~2 g DW m^{-2} day^{-1} were reported in 1972–1973 (Serruya et al. 1974; Serruya 1978) and in 2009–2011 (present study). We suggest that the enlarged GSR in the 1990s and earlier 2000s were triggered by exceptionally high water-level fluctuations, which caused massive redeposition of the historically settled particulate material to reach a new equilibrium with external forcing.

At peripheral locations, the measured GSRs were usually much higher and more variable than at Sta. A. The highest GSRs were recorded near the Jordan River inflow (Sta. J), where the contribution of allochthonous material delivered from the watershed is high. Shteinman et al. (2000) indicated that larger particles settle close to the river inflow and form a bar, while smaller particles are transported further into the lake. Vertical profiles of turbidity measured in spring along a transect from the Jordan River inflow to the lake center showed the presence of a thin (a few tens of centimeters) turbid water layer above the bottom (Ostrovsky unpublished). This suggests spreading of the fluvial material along the sloping bottom all the way down to the deepest part of the lake by gravity flow, following the model suggested for the dispersion of cold riverine water at the top of the thermocline or near the bottom (Serruya 1974).

27.2 Sedimentation of Particulate Inorganic Matter

Precipitation of $CaCO_3$ is the major sedimentation component of particulate inorganic material in Lake Kinneret. Spring decrease of alkalinity in the epilimnetic water indicates that the annual mean $CaCO_3$ sedimentation all over the lake ranges

Table 27.2 Comparison of published estimates of external loads of particulate matter

Source	Average load, t year^{-1}	Sedimentation rate[a], g DW m^2 day^{-1}	Method	Period	Reference
Jordan River inflow	74,000	1.2	Loads	1968–1970	Serruya (1971)
Jordan River inflow	70,000	1.2	Sediment traps	1971–1978	Inbar (1982)
Jordan River inflow	35,500 14,500	0.60 0.25	Loads Loads	1970–1987 1987–2011	Authors' assessment
Atmospheric deposition	10,000–16,000	0.16–0.26	Dust traps	1993–1996	Ganor et al. (2003)
Atmospheric deposition	10,000	0.17	Dust traps	2005	Chap. 19

[a] Average annual sedimentation rates of material exported from the Jordan River or as atmospheric deposits were calculated assuming equal distribution of loaded material over the whole lake area

from 0.7 to 1.4 g m^{-2} day^{-1}, which comprises 20–70 % of the sedimentation flux of inorganic particles measured at the center of the lake. Two allochthonous sources of inorganic particulate material should also be considered: (1) loads of suspended solids provided by rivers and creeks (the Jordan River is the dominant source of inorganic particles supplied from the watershed) and (2) dust (Table 27.2). Assuming a uniform distribution of the autochthonous and allochthonous particles over the lake bottom—the rates of particle contribution by the Jordan River, $CaCO_3$ precipitation, and dust settling were −0.52, 1.09, and 0.17 g m^{-2} day^{-1}, respectively, over the period from 1999 to 2011. Taking into account that the average sedimentation rate of inorganic material at Sta. A was 2.15 g m^{-2} day^{-1}, the three mentioned sources of inorganic material combined accounted for 83 % of the annual sedimentation flux of inorganic components. Taking into account uncertainties in appraisal of these components (e.g., part of fluvial particles is deposited near the river inlet zone; fine particles may be focused in the deeper part of the lake), this rough balance well portrays the main sources of sedimented material.

Previous studies suggested that material deposited at Sta. A contains, on average, about 50–60 % of $CaCO_3$, 23–36 % of silicates, and 14–25 % of POM (Serruya 1978; Klein and Koren 1998). The measurements carried out in 1999–2011 resulted in a higher proportion of POM of 33–42 %. The higher values may be partly explained by lesser diagenesis of organic particles in traps over a generally shorter time of their exposure (1–2 weeks in 1999–2011 vs. 2–4 weeks in earlier studies). Seasonal variations of trap material composition are event specific. A large proportion of POM in trap material is characteristic of the time of algal bloom collapse, while the inorganic fraction is usually high during a period of flood, which supplies particles from the watershed, and during spring precipitation of $CaCO_3$ (Koren and Ostrovsky 2002). Particles collected at shallower (peripheral) stations are characterized by 1.5–2 times lower percentage of POM than that at Sta. A. This is associated with wind- and internal wave-induced resuspension, which, on the one hand, washes the lighter particles out of the shallower areas and, on the other hand, delivers the organic-depleted resuspended particles to the traps (Ostrovsky et al. 1996; Ostrovsky and Yacobi 2010).

27.3 Sedimentation of Particulate Organic Matter

Organic matter sedimentation rates (OMSR), measured in the lake interior (Sta. A) by means of sediment traps positioned within the quiescent part of the hypolimnion, provide the most reliable assessments of POM fluxes from the upper productive layer into the deeper layers (Ostrovsky and Yacobi 2010). The POM sedimentation flux gradually declines from February until October (Fig. 27.2a). The ratio of this flux to primary production, called the export ratio (ER), shows the proportion of primary production settled from the upper productive layer. This ratio displays clear seasonality (Fig. 27.2b) that is related to the composition of the phytoplankton and

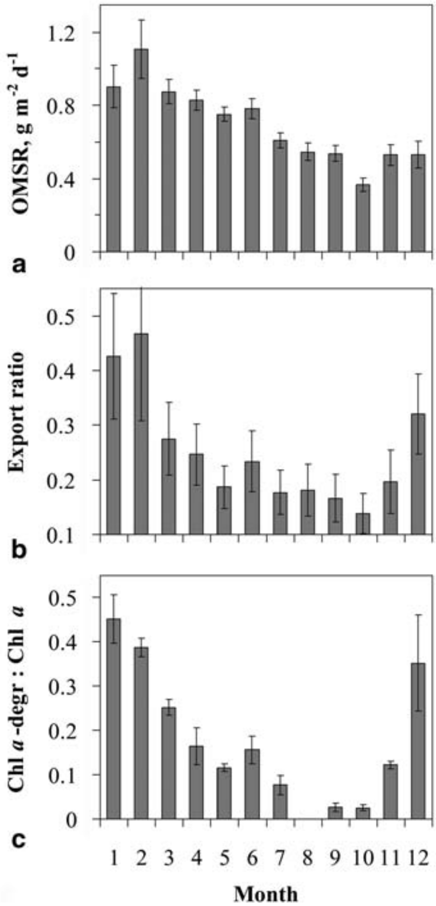

Fig. 27.2 The annual pattern of sedimentation parameters in Lake Kinneret. Means for 2005–2008: (**a**) organic matter sedimentation rate (*OMSR*), (**b**) export ratio, calculated as the ratio between the monthly averages of *OMSR* and primary production at Sta. A, and (**c**) mass ratio of chlorophyll degradation product sedimentation rate to chlorophyll *a* sedimentation rate (Chl *a*–degr: Chl *a*). Traps were positioned at ~11 m above the bottom to avoid oversampling of particulate material under turbulent conditions in the benthic boundary layer (Ostrovsky and Yacobi 2010). For details of primary production measurements, see elsewhere (Yacobi 2006). *Vertical bars* show ± standard error

to the physical regime in the lake. During holomixis (January–March), large-celled algae (e.g., the diatom *Aulacoseira granulata,* and the dinoflagellate *Peridinium gatunense*) dominate the phytoplankton and are hardly consumed by zooplankton (Zohary 2004). The high sinking velocity of such cells is an apparent reason why a high proportion of the phytoplankton reaches the lake bottom during warm winter days with low wind speeds when turbulent mixing is subtle. We assume that the temporal lag between algal production and sedimentation explains the highest proportion of POM in the settling material in February. Increased turbulence that prevails throughout the well-mixed water column entrains large algal cells and circulates them between the euphotic zone and the trap locations. The latter is apparently the reason for the overestimation of sedimentation flux of negatively buoyant particles in the non-stratified water column (Buesseler et al. 2007; Yacobi and Ostrovsky 2012). Loading of large amount of clay particles from the watershed and resuspension of particles from the bottom (specifically at the lake periphery) caused by surface waves on windy days explains the occurrence of organic-poor particles in the traps, and higher OMSR in winter and early spring. All these factors could account for the enlarged ER during complete (January–February) or partial holomixis (December). A prominent drop in ER occurs promptly after thermal stratification has established and the lower part of the water column becomes physically separated from the upper productive layer. Following the establishment of stable stratification, the ER declines from 27 to 18 % (Fig. 27.2b) and is explained by a shift in dominance in algal community from large to small slow-sinking phytoplankton species throughout the development of strong thermal stratification (Zohary 2004; Yacobi and Ostrovsky 2012). Development of buoyant filamentous cyanobacteria (e.g., *Aphanizomenon, Cylindrospermopsis*) in summer–fall since 1994 could also contribute to the seasonal decrease in the ER due to the floating capacity of these species (Walsby 1994). High turnover rates characteristic of small algal species also enhance nutrient recycling within the euphotic zone and may be the reason for the lowest rate of phosphorous loss from the epilimnion between July and November (Ostrovsky and Yacobi 2010). The seasonal timing of minimal ER and the greatest retention of limiting nutrients in the upper productive layer could be an outcome of universal adaptation of planktonic communities to stratification, when nutrient losses could not be replenished from internal or external sources. During the period of rapid thermocline deepening in late fall–early winter, large areas of the lake bottom, which were previously below the hypolimnion and where fresh organic particles had accumulated, now become overlain by the metalimnion or even the epilimnion. The interaction between internal waves, which are continuously presented in the metalimnion, with the exposed sediments cause massive resuspension of deposited fine particles and their lateral transportation toward the deepest part of the lake (Ostrovsky and Yacobi 1999; Ostrovsky 2000; Ostrovsky and Sukenik 2008). Such focusing of POM may explain high values of the ER computed for the end of the stratified period (Fig. 27.2b). The average ER of ~20 % apprised for the large part of the stratified period (March–October) when OMSR is the least biased at Sta. A is the best estimate for the export flux of the newly produced POM from the upper mixed layer. This value is typical for many productive lakes and the open ocean (Tilzer 1984; Baines et al. 1994; Bloesch and Uherlinger 1986; Laws et al. 2000; Ostrovsky and Yacobi 2010) and it probably reflects the adaptability of algal communities to varying ambient conditions.

27.4 Sedimentation and the Fate of Phytoplankton Pigments in the Water Column

A substantial component of POM is planktonic algae and their debris. The fate of this material can be traced by the examination of photosynthetic pigments in particles prevailing in water, traps, and bottom sediments (Hurley and Armstrong 1990; Leavitt and Hodgson 2003). Chlorophyll *a* (Chl *a*) is a pigment found universally in all oxygenic photosynthesizers (algae, cyanobacteria, and higher plants) and is usually used for quantification of phytoplankton biomass. Upon degradation, Chl *a* yields an array of degradation products, which reflect diagenetic processing of phytoplankton (Matile et al. 1999). Analysis of the seasonal variation of the ratio between Chl *a*-degraded products and intact Chl *a* in sediment traps helps to elucidate the trophic efficiency by which algal material in the water column is utilized (Ostrovsky and Yacobi 2010). This unitless ratio displayed similar seasonal dynamics in all traps, irrespective of their location, with maximum values of 0.4–0.6 during holomixis. The ratio had near-zero values from August to October (Fig. 27.2c), when the algal community consisted of small or buoyant species that possess low settling velocity (ca. tens of centimeters per day, Reynolds 2006) and are easily consumed by zooplankton, and thus can be readily recycled within the epilimnion (cf. low ER). The maximum values of the ratio during the holomixis are related to dominance of large algae, too big for consumption by zooplankton. These algae populate the entire water column such that a high proportion of their fragments may be maintained in the well-mixed turbulent water for a long time.

To better understand the fate of specific algal groups in the lake, a trap-to-water ratio (TWR) was developed (Yacobi and Ostrovsky 2008, 2012; Ostrovsky and Yacobi 2010). It compares pigment indices in the trap (PI_{trap}) and in the water of the upper productive stratum (PI_{water}), as follows

$$TWR = \frac{PI_{trap}}{PI_{water}} = \frac{F_i / F_{ref}}{C_i / C_{ref}}, \tag{27.1}$$

where F_i, F_{ref} are the fluxes (in mg m^2 day^{-1}) of the *i*th signature pigment and common reference pigment in trap, respectively; C_i, C_{ref} are the concentrations (in mg m^{-3}) of the *i*th signature pigment and reference common pigment in the upper productive stratum, respectively. Like Chl *a, β*-carotene (*β*-car) is found in all phytoplankton (save cryptophytes) and is thus suitable as a signature of total vegetative biomass. We preferred using *β*-car as a reference pigment, as this compound is the most stable algal pigment (Leavitt and Hodgson 2003). The TWR calculated on the

Table 27.3 Trap-to-water ratio (TWR) for different signature pigments in 2006

Pigment	Signature for	Jan–Mar (holomixis, oxic water)	Apr–Jun (stratified, suboxic hypolimnion)	Sep–Oct (stratified, anoxic hypolimnion)
Chl *a*	All algal groups	1.3	0.9	0.7
Chl *b*	Chlorophytes	*2.6*	*1.4*	*0.9*
Lutein + zeaxanthin	Chlorophytes (mainly)[a]	*2.6*	0.9	0.8
Fucoxanthin	Diatoms	*2.4*	0.3	0.4
Echineneone	Cyanobacteria	< 1	< 1	*0.5*
Peridinin	Dinoflagellates	0.5	*0.7*	Not in traps
Chl *c*	Dinoflagellates, diatoms	0.3	0.3	Not in traps

Ratios were calculated by Eq. (27.1) using β-carotene as a reference pigment (modified from Yacobi and Ostrovsky 2008). Numbers in italics refer to dominant algal groups

[a] In this study, lutein (a signature pigment of chlorophytes) could not be analytically separated from zeaxanthin (a signature pigment of cyanobacteria). From January to June the mixture of these pigments reflect primarily chlorophytes since cyanobacteria were presented only in minor quantities (Yacobi and Ostrovsky 2008). This was also supported by a high correlation ($r^2 > 0.9$) between concentrations of lutein + zeaxanthin and Chl *b* (indicatory of chlorophytes) in the samples

basis of *β*-car reflects the "freshness" of the newly settled algal material relative to that in the euphotic zone.

We calculated the TWR for pigments that are signatures of phytoplankton groups (Table 27.3). Although TWR changed in the three defined periods, the stability of phytopigments appears as follows: β-carotene > lutein > Chlorophyll *b* (Chl *b*) > Chl *a* > fucoxanthin > echinenone > Chlorophyll *c* (Chl *c*) > peridinin (Yacobi and Ostrovsky 2008). This pattern agrees with results reported earlier (e.g., Hurley and Armstrong 1990; Leavitt and Hodgson 2003) and suggests the following order of algal preservation: chlorophytes > diatoms > cyanobacteria > dinoflagellates. Chl *c* displayed the same pattern of degradability as peridinin reflecting a fast decomposition of dinoflagellates in the water column although sometimes dinoflagellates reach traps intact (Zohary et al. 1998). Fucoxanthin was harbored mainly by diatoms, which formed high concentrations in February, in June–July, and in September–November. Abrupt appearance and disappearance of the large centric diatom *Aulacoseira granulata* is typical in winter. The species sinks massively, such that a large part of the sinking population includes intact cells and determines high TWR for fucoxanthin. In contrast, low TWR values for fucoxanthin in the summer and autumn were associated with the dominance of small pennate diatoms (Zohary 2004) which have low thinking velocity; they are consumed by zooplankton and decompose mainly within the epilimnion. Chl *b* and lutein showed a prominent peak in March–April, when relatively dense population of chlorophytes were eliminated from the euphotic zone. The high TWR of Chl *b* and lutein indicates that chlorophyte, or debris originating in chlorophyte cells, accumulated in the traps in higher rates than other algae that prevailed simultaneously in the epilimnion (Yacobi and Ostrovsky 2012). During the stratified period, the TWR for Chl *b* and lutein are slightly below 1, indicating better preservation of chlorophyte cells comparatively to other phytoplankton groups. Echinenone TWR was mostly < 1 during the holomixis and consistently low when the lake was stratified (Yacobi and Ostrovsky 2008). This indicates that echinenone is less stable than the signature pigments of the chlorophytes and suggests that cyanobacteria recycle mainly in the upper part of the water column. Thus, TWR > 1 is characteristic for most pigments during holomixis when algal cells settle down intact, while TWR < 1 is characteristic of pigments in a stratified lake and suggests that cells mostly decompose in the epilimnion before reaching the bottom (Yacobi and Ostrovsky 2008, 2012). These temporal changes in TWR concur with the above described dynamics of Chl *a*-degraded products and ER, as large individual cells may have better ability to survive in the deep non-stratified water column with limited light, while the ability to retain and recycle in the upper euphotic layer under conditions of nutrient limitation may well confer an evolutionary advantage to small or buoyant algal populations.

27.5 The Burial of Sedimented Particles

Sediment accumulation (= burial) rate, SAR, can be most reliably assessed from sedimentation flux estimates at Sta. A, because recurrently resuspended material have minimal influence on trap measurements at this deep station (Ostrovsky and Yacobi 2010). The computed SAR indicated twofold variations over the last decade: from 2.5–3 mm $year^{-1}$ during the drought of 2008–2011 to 5.7 mm $year^{-1}$ in the rainy 2003. The mean SARs based on trap measurements for the 1990s and early 2000s (4–5 mm $year^{-1}$) well agree with sediment core dating (Table 27.4). Sobek et al. (2011) found that SAR near the Jordan inlet (Sta. J) is ~1.5 times higher than at the lake center. On the other hand, at peripheral stations, SARs are 1.5–2 times lower than that at Sta. A. The latter corroborates our conclusion about relocation of sedimented particles from shallow areas toward the lake center (Ostrovsky and Yacobi 1999, 2010). Gradual increase in organic matter content in the uppermost (few millimeters) layer of bottom sediments from the littoral to the lake center (Ostrovsky and Yacobi 1999; Yacobi and Ostrovsky 2000) supports the notion of focusing of lighter organic-rich particles in the deep part of the lake. At the same time, much lower content of organic material in the uppermost layer during holomixis in comparison with the stratified period suggests seasonal dissimilarity in chemical and physical processes influencing the fate of settling and decomposition of organic and inorganic particles in the water column. In particular, internal seiching strongly influences the sedimentation regime during the stratified period (Ostrovsky et al. 1996, 1997; Ostrovsky and Yacobi 2010).

Overall, the dynamic sedimentation processes ultimately affect the amount of suspended organic and inorganic material, concentrations of nutrients and pollutants in the upper productive stratum by means of their export to lower strata and bottom sediments. The anthropogenic increase in water demands and reduction of precipitation in the region during the past decades altered the hydrological regimes and material load from the watershed to Lake Kinneret (Ostrovsky et al. 2013; Chaps. 7 and 18). Such changes concurrently with the increase beyond natural in

Table 27.4 Sediment accumulation rates

Location	Accumulation rate, mm $year^{-1}$	Method	Layer location in sediments	Period	Reference
Sta. A	2.8	^{137}Cs profiles	Surface layer	–	Stiller and Assaf (1973)
PS	2.0–5.1	^{137}Cs profiles	Surface layer		Stiller and Assaf (1973)
Sta. A	3.5	Sediment trap	Surface layer	1990–1992	Nishri and Koren (1993)
Sta. A	4	^{137}Cs profiles	Surface layer	Recent	Nishri and Koren (1993)
KINU8	4.7	^{210}Pb dating	0–5 cm	1982–1993	Erel et al. (2001)
	5.0	and $\delta^{13}C_{org}$ ED	5–12 cm	1959–1982	Erel et al. (2001)
	7.1		12–33 cm	1953–1959	Erel et al. (2001)
KINU8	4.3	$\delta^{13}C_{org}$ ED	0–11 cm	1975–1993	Dubowski et al. (2003)
	5.6	and	11–25 cm	1950–1975	Dubowski et al. (2003)
	6.1	C_{org} content	25–59 cm	1872–1950	Dubowski et al. (2003)
Sta. A	3.6	^{210}Pb	0–40 cm	1890–2002	Hambright et al. (2004)
Sta. A	4.5	Mixed	0–10 cm	Recent	Sobek et al. (2011)
PS	2.0–2.8	^{210}Pb and ^{137}Cs	0–10 cm	Recent	Sobek et al. (2011)
Sta. J	6.1		0–10 cm	Recent	Sobek et al. (2011)
Sta. A	4.3 ± 0.7[a]	Sediment trap	Surface layer	1999–2007	Present study
Sta. A	2.6 ± 0.3[a]	Sediment trap	Surface layer	2008–2011	Present study

Accumulation rates are presented as means and ranges, or means ± SD
KINU8 is a sampling station located ~2 km northwest of Sta. A, *PS* are peripheral stations, *δ^{13} C_{org} ED* is event dating using δ^{13} C. Locations of Sta. A and Sta. J are indicated in Fig. 32.1, Chap. 32
[a] Calculations are based on specific gravity of ash fraction = 2.65 g cm^{-3} and organic matter fraction = 1 g cm^{-3}; porosity in the upper 10-cm layer = 87 % (Sobek et al. 2011)

the amplitude of water-level fluctuations as well as long-term water-level decline influenced the algal community and modified the GSRs and material redeposition in the lake.

References

Baines SB, Pace ML, Karl DM (1994) Why does the relationship between sinking flux and planktonic primary production differ between lakes and oceans? Limnol Oceanogr 39:213–226

Bloesch J (2004) Sedimentation and lake sediment formation. In: O'Sullivan PE, Reynolds CS (eds) The lakes handbook, vol 2: lake restoration and rehabilitation. Blackwell, Malden, pp 197–229

Bloesch J, Uehlinger U (1986) Horizontal sedimentation differences in a eutrophic Swiss lake. Limnol Oceanogr 31:1094–1109

Buesseler KO, Lamborg CH, Boyd PW, Lam PJ, Trull T, Bidigare RR, Bishop JKB, Casciotti KL, Dehairs F, Elskens M, Honda M, Karl DM, Siegel DA, Silver MW, Steinberg DK, Valdes J, VanMooy B, Wilson S (2007) Revisiting carbon flux through the ocean's twilight zone. Science 316:567–570

Dubowski Y, Erez J, Stiller M (2003) Isotopic paleolimnology of Lake Kinneret. Limnol Oceanogr 48:68–78

Eckert W, Didenko J, Uri E, Eldar D (2003) Spatial and temporal variability of particulate phosphorus fractions in seston and sediments of Lake Kinneret under changing loading scenario. Hydrobiologia 494:223–229

Erel Y, Dubowski Y, Halicz L, Erez J, Kaufman A (2001) Lead concentrations and isotopic ratios in the sediments of the Sea of Galilee. Environ Sci Technol 35(2):292–299

Ganor E, Foner HA, Gravenhorst G (2003) The amount and nature of the dustfall on Lake Kinneret (the Sea of Galilee), Israel: flux and fractionation. Atmos Environ 37:4301–4315

Håkanson L, Jansson M (1983) Principles of lake sedimentology. Springer, Berlin

Hambright KD, Eckert W, Leavitt PR, Schelske CL (2004) Effects of historical lake level and land use on sediment and phosphorus accumulation rates in Lake Kinneret. Environ Sci Technol 38:6460–6467

Hurley JP, Armstrong DE (1990) Fluxes and transformations of aquatic pigments in Lake Mendota, Wisconsin. Limnol Oceanogr 35:384–398

Inbar M (1982) Measurement of fluvial sediment transport compared with lacustrine sedimentation rates: the flow of the River Jordan into Lake Kinneret. Hydrol Sci J 27(4):439–449

Klein M, Koren N (1998) The influence of the thermocline on sedimentation in the deeper part of Lake Kinneret, Israel. Limnologica 28:293–299

Koren N, Klein M (2000) Rate of sedimentation in Lake Kinneret, Israel: spatial and temporal variations. Earth Surf Proc Landf 25:895–904

Koren N, Ostrovsky I (2002) Sedimentation in a stratified subtropical lake. Verh Int Ver Theor Angew Limnol 27:2636–2639

Laws EA, Falkowski PG, Smith WO, Ducklow H, McCarthy JJ (2000) Temperature effects on export production in the open ocean. Global Biogeochem Cycle 14(4):1231–1246

Leavitt PR, Hodgson DA (2003) Sedimentary pigments. In: Smol JP, Birks HJB, Last WM (eds) Tracking environmental changes using lake sediments, vol 3: terrestrial, algal, and siliceous indicators. Kluwer, Dordrecht, pp 295–325

Matile P, Hörtensteiner S, Thomas H (1999) Chlorophyll degradation. Annu Rev Plant Physiol Plant Mol Biol 50:67–95

Nishri A, Koren N (1993) Sediment transport in Lake Kinneret. Verh Int Ver Theor Angew Limnol 25:290–292

Ostrovsky I (2000) The upper most layer of bottom sediments: sampling and artifacts. Ergeb Limnol 55:243–256

Ostrovsky I, Sukenik A (2008) Spatial heterogeneity of biogeochemical parameters in a subtropical lake. In: Mohanty PK (ed) Monitoring and modeling lakes and coastal environments. Springer, Dordrecht, The Netherland, pp 79–90

Ostrovsky I, Yacobi YZ (1999) Organic matter and pigments in surface sediments: possible mechanisms of their horizontal distributions in a stratified lake. Can J Fish Aquat Sci 56:1001–1010

Ostrovsky I, Yacobi YZ (2010) Sedimentation flux in a large subtropical lake: spatio-temporal variations and relation to primary productivity. Limnol Oceanogr 55:1918–1931

Ostrovsky I, Yacobi YZ, Walline P, Kalikhman I (1996) Seiche induced mixing: its impact on lake productivity. Limnol Oceanogr 41:323–332

Ostrovsky I, Wynne D, Bergstein-Ben Dan T, Nishri A, Li H, Yacobi YZ, Koren N, Parparova R (1997) Spatial distributions of biogeochemical parameters in surface sediments at the beginning of the stratified period in a subtropical lake. Water Air Soil Pollut 99:497–505

Ostrovsky I, Rimmer A, Agnon Y, Koren N (2006) Sediment resuspension in the hypolimnion of Lake Kinneret (Israel): the impact of water level fluctuation. Verh Int Ver Theor Angew Limnol 29:1625–1629

Ostrovsky I, Rimmer A, Yacobi YZ, Nishri A, Sukenik A, Hadas O, Zohary T (2013) Long-term changes in the Lake Kinneret ecosystem: the effects of climate change and anthropogenic factors. In: Goldman CR, Kumagai M, Robarts RD (eds) Climate change and inland waters: impacts and mitigation approaches for ecosystems and society. Wiley-Blackwell, Oxford, UK, pp 271–293

Reynolds CS (2006) Ecology of phytoplankton. Cambridge University Press, Cambridge

Rimmer A, Gal G, Opher T, Lechinsky Y, Yacobi YZ (2011) Causes for long-term variations of thermal structure in a warm lake. Limnol Oceanogr 56:974–988

Serruya C (1971) Lake Kinneret: the nutrient chemistry of the sediments. Limnol Oceanogr 16:510–521

Serruya S (1974) The mixing patterns of the Jordan River in Lake Kinneret. Limnol Oceanogr 19:175–181

Serruya C (1978) Sediment chemistry. In: Serruya C (ed) Lake Kinneret, momographiae biologicae. Junk, Amsterdam, pp 205–215

Serruya C, Edelstein M, Pollingher U, Serruya S (1974) Lake Kinneret sediments: nutrient composition of the pore water and mud water exchanges. Limnol Oceanogr 19:489–508

Shteinman B, Wynne D, Kamenir Y (2000) Study of sediment dynamics in the Jordan River-Lake Kinneret contact zone using tracer methods. The hydrology–geomorphology interface: rainfall, floods, sedimentation, land use. Proceedings of the Jerusalem Conference, May 1999. IAHS Publ. 261, pp 275–284

Sobek S, Zurbrügg R, Ostrovsky I (2011) The burial efficiency of organic carbon in the sediments of Lake Kinneret. Aquat Sci 73:355–364

Stiller M, Assaf G (1973) Sedimentation and transport in Lake Kinneret traced by ^{137}Cs. In: Hydrology of lakes. Proceedings Helsinki Symposium, July 1973. IAHS Publ. 109, pp 397–403

Tilzer MM (1984). Estimation of phytoplankton loss rates from daily photosynthetic rates and observed biomass changes in Lake Constance. J Plankton Res 6:309–324

Walsby AE (1994) Gas vesicles. Microbiol Rev 58:94–144

Wassmann P (2004) Eutrophication, primary production and vertical export. In: Wassmann P, Olli K (eds) Drainage basin nutrient inputs and eutrophication: an integrated approach. University of Tromsø, Norway, pp 126–138 (available at http://hdl.handle.net/10037/2389)

Yacobi YZ (2006) Temporal and vertical variation of chlorophyll a concentration, phytoplankton photosynthetic activity and light attenuation in Lake Kinneret: possibilities and limitations for simulation by remote-sensing. J Plankton Res 28:725–736

Yacobi YZ, Ostrovsky I (2000) Lake Kinneret sediments: spatial distribution of chloropigments during holomixes. Arch Hydrobiol 55:457–469

Yacobi YZ, Ostrovsky I (2008) Downward flux of organic matter and pigments in Lake Kinneret (Israel): relationships between phytoplankton and the material collected in sediment traps. J Plankton Res 30:1189–1202

Yacobi YZ, Ostrovsky I (2012) Sedimentation of phytoplankton: role of ambient conditions and life strategies of algae. Hydrobiologia 698:111–120

Zohary T (2004) Changes to the phytoplankton assemblage of Lake Kinneret after decades of predictable repetitive pattern. Freshw Biol 49:1355–1371

Zohary T, Ostrovsky I (2011) Ecological impacts of excessive water level fluctuations in stratified freshwater lake. Inland Waters 1:47–59

Zohary T, Pollingher U, Hadas O., Hambright KD (1998) Bloom dynamics and sedimentation of *Peridinium gatunense* in Lake Kinneret. Limnol Oceanogr 43:175–186